ELSEVIER

Intermetallics 8 (2000) 945–951

Intermetallics

www.elsevier.com/locate/intermet

Distribution behaviour of alloying elements in $\alpha_2(\alpha)/\gamma$ lamellae of TiAl-based alloy

G.W. Qin [a,*], G.D.W. Smith [b], B.J. Inkson [b], R. Dunin-Borkowski [b]

[a] *Materials Engineering Division, Tohoku National Industrial Research Institute, Sendai 983, Japan*
[b] *Department of Materials, University of Oxford, Parks Road, Oxford OX1 3PH, UK*

Received 6 March 2000; received in revised form 18 May 2000; accepted 18 May 2000

Abstract

Primary $\alpha_2(\alpha)/\gamma$ lamellae structure in a Ti–47Al–2Nb–1Cr–1V alloy (in at.%) was obtained depending on different cooling rates from the high-temperature α single phase region after the alloy was solution treated there. Atom probe (AP) microanalysis and TEM with electron energy loss spectroscopy (EELS) were run to examine the partitioning behaviour of Nb, Cr, V, O and C in the high-temperature α/γ lamellae. The results show that V and Cr, and interstitial elements C and O are enriched in the high-temperature α phase, while Nb is homogeneous in the two phases. The EELS result qualitatively agrees with that of AP microanalysis. No segregation of these alloying elements was detected along the observed high-temperature α/γ interface.

Keywords: A. Titanium aluminides, based on TiAl; B. Phase transformations; D. Phase interfaces; F. Atom microprobe

1. Introduction

The presence of a small amount of α_2 phase in γ-TiAl-based ($\gamma+\alpha_2$) alloy produces a lamellar structure which is very important for improved strength and toughness [1–5]. In order to improve its comprehensive mechanical properties, especially the brittleness at room temperature, extensive research efforts for this candidate aerospace material over the past decade have been focused on alloying additions of Nb, Cr, V and etc [3,5–10]. These elements are well known to improve the ductility [8,9] and Nb also to improve the oxidation resistance [11].

Up to date, numerous transformation modes related to the formation of this kind of α_2/γ lamellar structure (L), $\alpha\rightarrow L(\alpha/\gamma)\rightarrow L(\alpha_2/\gamma)$, $\alpha\rightarrow\alpha_2\rightarrow L(\alpha_2/\gamma)$ or $\gamma\rightarrow L(\alpha/\gamma)\rightarrow L(\alpha_2/\gamma)$, have been widely identified [8,12–14]. However, the precipitation mechanism of $\alpha_2(\alpha)/\gamma$ lamellae, a diffusional or shear process, is still in question [12–20], and, especially, there is very limited understanding of the partitioning behaviour of alloying elements in $\alpha_2(\alpha)$ and γ phases in primary lamellar structure or in the lamellar structure after a long-term exposure at high temperature, as well as their segregation along α_2/γ and γ/γ interfaces at the atomic scale [17,19,21–26]. In this study, an engineering candidate material, Ti–47Al–2Nb–1Cr–1V alloy (nominal composition at atomic percentage), has been run to examine these contents by AP microanalysis and TEM with EELS.

2. Experimental procedure

A Ti–47Al–2Nb–1Cr–1V alloy was prepared by consumable electrode arc-melting, and then forged isothermally at 1000°C for over 50% plastic strain (see [9] for details). The alloy was solution treated at 1400°C for 15 min, and then cooled to 1300°C at a rate of 50^0C/min, or cooled to 850°C at 5°C/min, followed by water quenching to room temperature. The later treated sample was finally annealed at 800°C for 216 h, followed by water quenching to room temperature.

AP specimens were made by the standard two-stage electropolishing process [22]. Atom probe field ion

* Corresponding author. Tel.: +81-22-237-5211; fax: +81-22-236-6839.
E-mail address: gwqin@tniri.go.jp (G.W. Qin).

0966-9795/00/$ - see front matter
PII: S0966-9795(00)00070-4

microscopy (AP-FIM) study was carried out by using the optical position sensitive atom probe (PoSAP) instruments at Oxford, with imaging gas of Ne at 2×10^{-3} Pa for FIM observation, and with high vacuum at about 7×10^{-9} Pa for AP microanalysis with a pulse fraction of 18% to DC voltage and tip temperature of 70 K. TEM observation and EELS analysis were carried on the JEOL 3000F field-emission transmission electron microscope.

During AP microanalysis, titanium, aluminum, and the alloying elements were mainly detected as doubly charged ions, as shown in Fig. 1. As for the calculation of the total concentration of the alloying elements, mass peaks of $^{50}Cr^{2+}$ and $^{54}Cr^{2+}$ overlap that of $^{50}Ti^{2+}$ and $^{50}V^{2+}$, and $^{27}Al^{+}$, as shown in Fig. 1, but according to the isotope abundance ratio, the natural abundance of $^{50}Cr^{2+}$, $^{54}Cr^{2+}$ and $^{50}V^{2+}$ is only 4.31, 2.38 and 0.25%, respectively. So the mean error of the Cr and V content in this alloy derived from the neglect of $^{50}Cr^{2+}$, $^{54}Cr^{2+}$ and $^{50}V^{2+}$ is less than 0.07 and 0.003 at.% in total, respectively.

3. Experimental results and discussion

3.1. Microstructure of the alloy

For the forged alloy, the as-cast fully α_2/γ lamellae become equiaxed and refined due to dynamic recrystallization during the isothermal forging process, and the equiaxed α_2 and γ particles are small in size of 2–10 μm (Fig. 2a) [9]. After the alloy was solution treated at 1400°C (in the α single phase region [8,9]) and then cooled, large lamellar colony with size of 2–3 mm was developed, as shown in Fig. 2b and c, which suggests that the transformations of $\alpha_2\rightarrow\alpha$ and $\gamma\rightarrow\ \gamma+\alpha\rightarrow\alpha$ [8] are very rapid from previous small equiaxed α_2 and γ particles at 1400°C, and the transformed small α grains coalesce into the large-size ones (2–3 mm) accompanying with composition homogenization of the alloy.

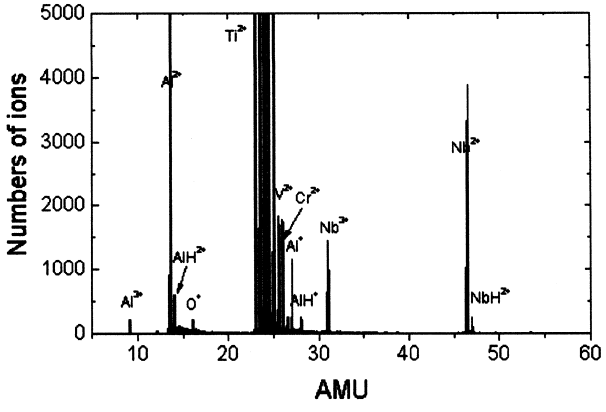

Fig. 1. Atom probe mass spectrum of the alloy treated at 1400°C for 15 min, and then cooled to 1300°C at 50°C/min, followed by water quenching to room temperature.

When the alloy was cooled from 1400 to 1300°C, the α and γ lamellae precipitated from the supersaturated α grains produce the fully lamellar structure (*primary α/γ lamellae*) with fine interlamellar spacing, and also with about 1–2 vol.% small equiaxed grains along lamellar colony boundary due to coarsening of the tips of primary lamellae during the lamellae precipitation [27], as shown in Fig. 2b. The high-temperature α transforms into α_2 phase after quenching because the $\alpha\rightarrow\alpha_2$ disorder/order transformation takes place [8,12–15]. If the alloy was cooled to 850°C and then annealed at 800°C for 216 h, except a little more equiaxed grains with larger size along the lamellar colony boundaries, the fully lamellar structure (Fig. 2c) does not change its morphology and is very similar as Fig. 2b. The X-ray diffraction result confirms the lamellar structure is composed of only α_2 and γ phases, but the volume fraction of α_2 phase varies with the heat treatment schedules, the more occurring after the rapid cooling of 1400→1300°C and the less after the slow cooling to 850°C and the following annealing at 800°C (less than 5 vol.%).

3.2. Partitioning behaviour of the alloying elements in $\alpha_2(\alpha)/\gamma$ lamellae

The poles in the FIM image of the γ phase were well observed while not in that of the α_2 phase, which might be due to a lower ordering degree of the α_2 phase [22], as shown in Fig. 3. For the alloy cooled from 1400 to 1300°C, the AP microanalyzed region of about 15×15 nm was selected, as shown by the dashed square in Fig. 3a. Several hours later, after the simultaneous observation showed a composition jump at a $\alpha_2(\alpha)/\gamma$ interface (Fig. 4B), the FIM observation showed the image of the α_2 phase (Fig. 3b), which was in good agreement with the AP composition analysis.

The further AP results show that V and Cr, and interstitial elements C and O are enriched in the $\alpha_2(\alpha)$ phase, while Nb is almost homogeneous in the two phases. The EELS results are also qualitatively consistent with that of the AP microanalysis, as shown in Fig. 5. The compositions of primary α_2 and γ lamellae in the alloy are listed in Table 1, together with the partitioning coefficients $K_i^{\alpha2(\alpha)/\gamma}$ (i=Nb,Cr,V) for each alloying element, which is consistent with the previous studies about Nb- and Cr-doped TiAl alloys [23–25,28]. The α_2 phase absorbs strongly impurities such as C and O to purify alloy [21,22], and results possibly in improved mechanical properties of alloys [29,30].

In the case of α/γ phase equilibrium with several atomic percentages of additive(s) in a Ti–Al–*i* system, γ phase-stabilizing parameter $\Delta^{*}G_i^{\alpha\rightarrow\gamma}$ can be expressed by [28,31]

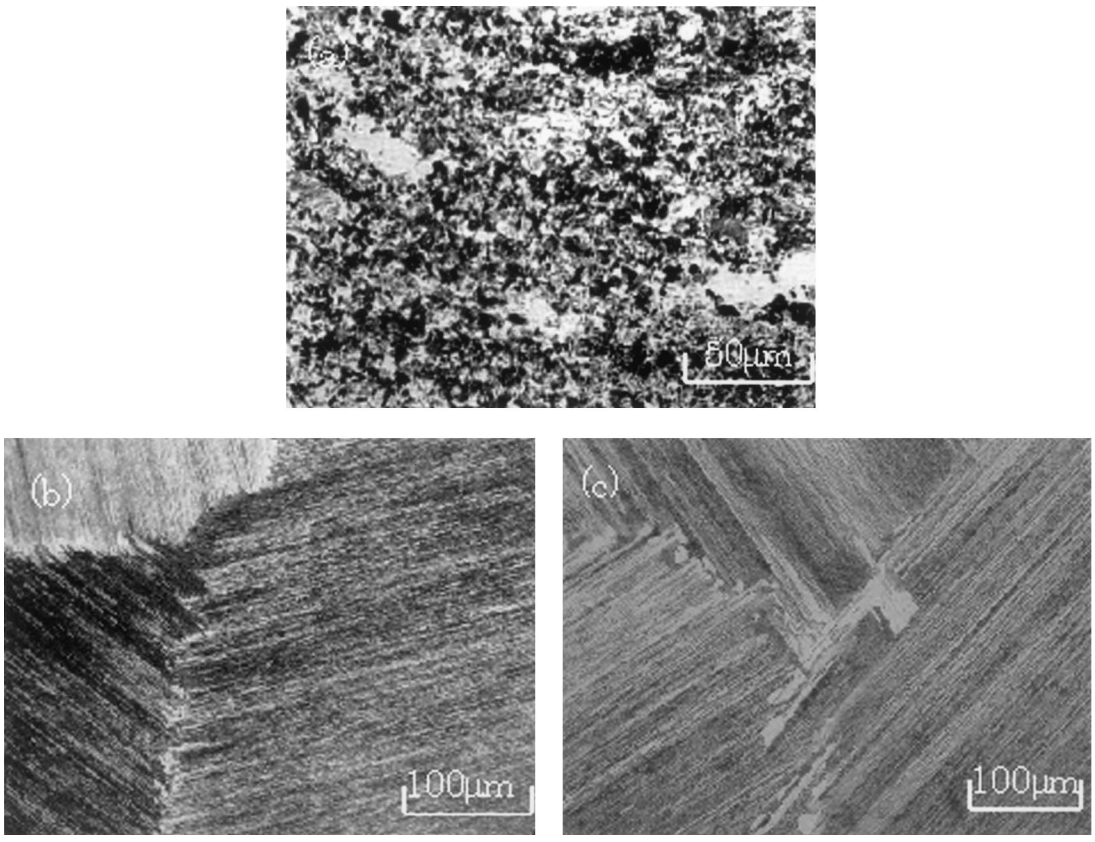

Fig. 2. Optical micrographs of the Ti–47Al–2Nb–1Cr–1V alloy: (a) fine equiaxed ($\alpha_2+\gamma$) two-phase microstructure after the alloy was isothermally forged [9]; (b) and (c) fully lamellar structures of the alloy solution treated at 1400°C for 15 min: (b) cooled to 1300°C at 50°C/min, followed by water quenching (WQ) to room temperature; (c) cooled to 850°C at 5°C/min, further annealed at 800°C for 216 h, followed by WQ, showing a little more equiaxed grains at the lamellar colony boundaries due to lamellae coarsening [27].

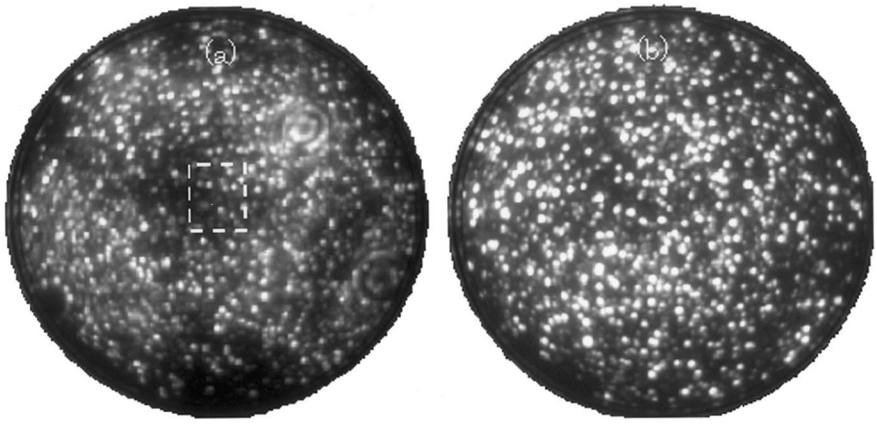

Fig. 3. FIM images of the Ti–47Al–2Nb–1Cr–1V alloy cooled from 1400 to 1300°C at 50°C/min and then WQ: (a) showing a single γ phase before AP microanalysis; (b) showing a single $\alpha_2(\alpha)$ phase after AP microanalysis. Both images were taken at a temperature of 70 K with the voltages of (a) 9.1 KV, (b) 10.8 KV.

$$\Delta^{*}G_i^{\alpha\rightarrow\gamma} = RT\ln K_i^{\alpha/\gamma} \quad (1)$$

where R is the gas constant and T the absolute temperature. The $\Delta^{*}G_i^{\alpha\rightarrow\gamma}$ value indicates the effect of the additive(s) i on the thermodynamic stability of γ or α phase depending on its negative or positive character. In this study, therefore, the partitioning behaviour also suggests that Cr and V prefer to stabilize high-temperature α phase [28] while Nb has little preference.

Because the thermodynamic character of V is very similar as that of Cr in this system [9], if compared with the equilibrium compositions of the α and γ phases in a

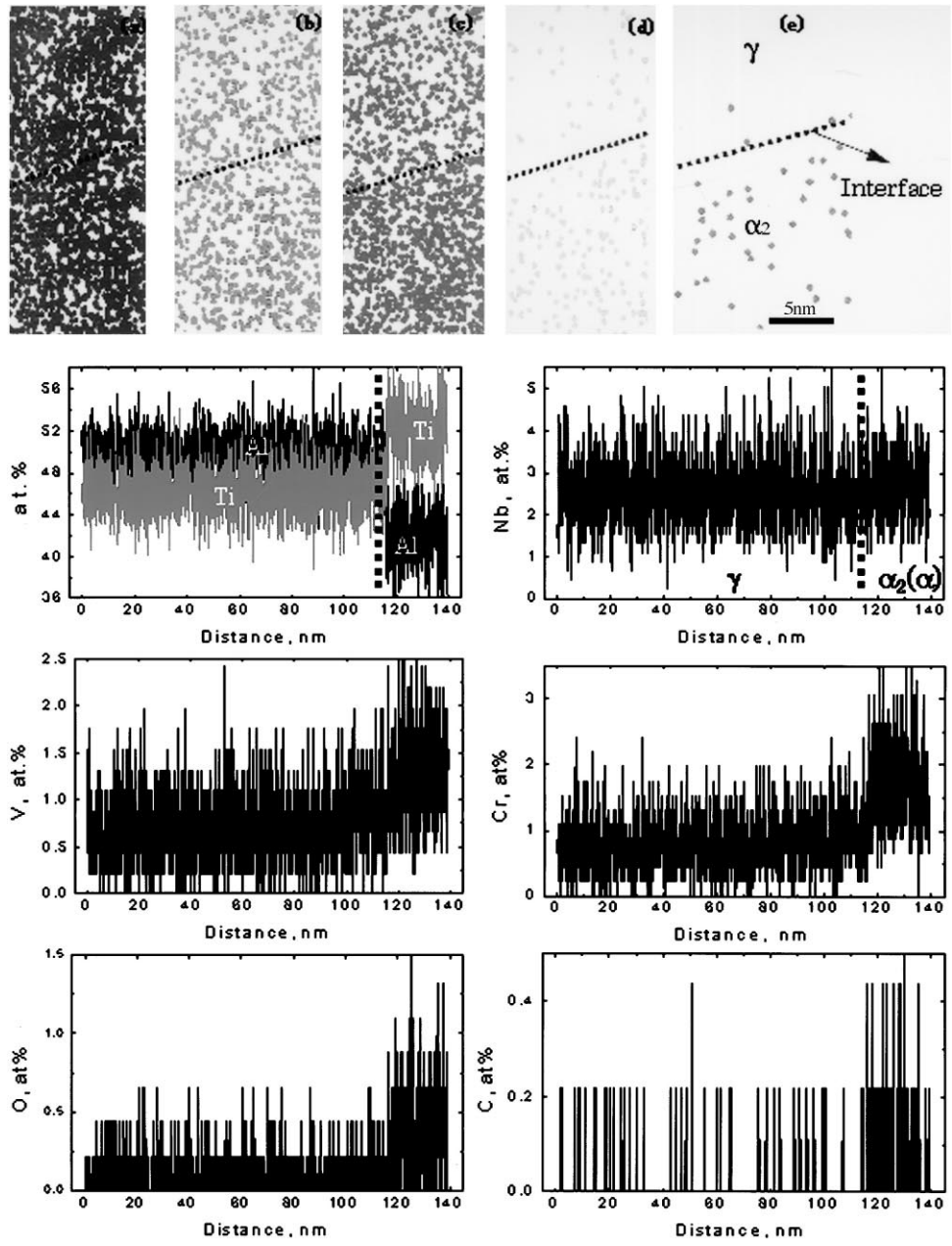

Fig. 4. (A) The reconstructed atom maps of the solute partitioning across primary $\alpha_2(\alpha)/\gamma$ interface for Ti–47Al–2Nb–1Cr–1V alloy cooled from 1400 to 1300°C at 50°C/min: (a) Nb; (b) V; (c) Cr; (d) O; (e) C. (B) The composition profile across the primary $\alpha_2(\alpha)/\gamma$ interface corresponding to (A).

Ti–48Al–2Nb–2Cr alloy (in at.%) at 1300°C obtained by electron probe microanalysis (EPMA) [28], the AP result is similar as the EPMA result. It also means that the compositions of primary α and γ phases approach easily to equilibrium during their rapid precipitation in the supersaturated α matrix. This result is consistent with that by Hono et al. [20] and Tanimura et al. [17] using Ti–Al binary alloys.

The significant composition difference between the two phases of high-temperature primary α/γ lamellae, further suggests that it is possible for the α/γ lamellae to precipitate through a diffusional process. If in this case, the thickness of γ lamellae precipitated in the high-temperature α matrix, X, can be expressed by [32]

$$X = \left[\frac{(C_0 - C_\alpha)^2}{(C_\gamma - C_\alpha)(C_\gamma - C_0)}\right]^{1/2} (Dt)^{1/2} \quad (2)$$

where D is the interdiffusion coefficient of Ti and Al in high temperature α matrix, and t the diffusion time. The C_0, C_α and C_γ are the concentrations of the alloy, the precipitated α and γ phases, respectively, and here

assuming $C_\gamma > C_\alpha$. For the alloy cooled from 1400 to 1300°C, if $D = 1.1\times10^{-13}$ m^2/s at 1300°C [33] and $t = 60$ s are taken, and if the above concentrations are treated as that of Al or Ti element, X is roughly equal to 4.6 or 1.4 μm, respectively. The observed value (about 0.1–0.2 μm) of the interlamellar spacing (Fig. 5) is less than the calculated result, but here it should be noted that the calculation above is the maximum case because the following influences are not considered in the calculation due to the lack of many dynamic data in this system: (1) the overlapping of the diffusion fields between one γ lamella and the adjacent one [32]; (2) the precise evaluation of the diffusion time t; (3) the possible decrease of the interdiffusivity due to the alloying additions [34]. All of these factors will decrease the above-calculated thickness, especially the first one does drastically [32]. Hence, it is reasonable for this discrepancy between the estimated value and the observed one.

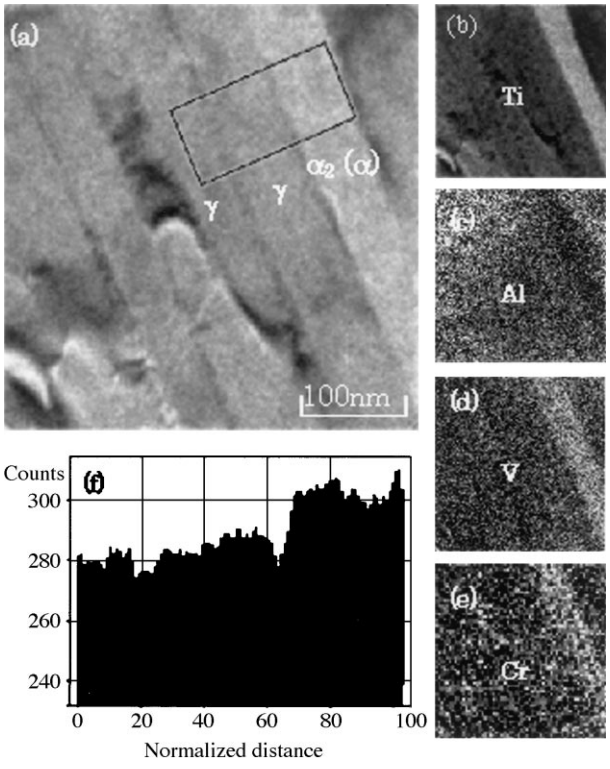

Fig. 5. TEM bright field micrograph (a) imaged in the [1$\bar{1}$0] orientation showing primary $\alpha_2(\alpha)/\gamma$ lamellar structure precipitated in the high-temperature α matrix for the alloy cooled from 1400 to 1300°C at 50°C/min and followed by water quenching to room temperature, the corresponding EELS maps (b)–(e) of each element except Nb due to much noise, and (f) the intensity distribution of Ti element in the marked region of (a).

Actually, when the alloy was cooled from 1400 to 1300°C, a large driving force of γ phase precipitation due to the high Al content makes γ lamellae nucleate homogeneously and closely [14], resulting in the diffusion fields overlapping. And the precipitated α, γ and γ twin impinge on each other before they can become thicker and finally produce this fine lamellar structure.

As for the evaluation of the diffusion time, a metastable transformation ($\alpha\rightarrow\alpha+\gamma$) line (T-line) was introduced [8], and the T-line temperature is very sensitive to the cooling rate and it decreases by about 70°C for a Ti–47Al alloy at a cooling rate of 100°C/min. The α transus temperature is about 1350°C for this alloy [8], so the precipitation time of primary α/γ lamellae in our case should be much less than 60 s, and would probably be several to tens of seconds.

Therefore, it is acceptable for the observed value being less than the estimated maximum one, and it shows indeed that the precipitation of primary α/γ lamellae in the high temperature α matrix is probably controlled by a diffusional process and the compositions of the two phases are easy to get into equilibrium during the thickening of the γ lamellae if combined with an

Table 1
The compositions of $\alpha_2(\alpha)$ and γ phases across $\alpha_2(\alpha)/\gamma$ interface (in at.%)

Temperature	Phase	Al	Ti	Nb	V	Cr	O	C	$K_{Nb}^{\alpha2/\gamma}$	$K_{V}^{\alpha2/\gamma}$	$K_{Cr}^{\alpha2/\gamma}$
1400→1300°C	$\alpha_2(\alpha)$	41.1	52.1	2.9	1.5	1.9	0.4	0.06	1.0	1.9	2.1
	γ	48.5	46.8	2.9	0.8	0.9	0.1	0.01			
1300°C [28]	$\alpha_2(\alpha)$	43.4	51.7	2.0		2.9			≈1.0		1.6
	γ	48.8	47.3	2.1		1.8					
850°C[a]	α_2										
	γ	46.4	49.1	2.8	0.8	0.8	0.08	0.02			
800°C[a]	α_2										
	γ	45.3	49.8	3.0	0.8	1.0	0.06	0.01			
1000°C [28]	α_2	35.4	60.6	1.8		2.2			0.7		1.0
	γ	46.3	49.1	2.6		2.2					

[a] 850°C means the Ti–47Al–2Nb–1Cr–1V alloy cooled from 1400 to 850°C at 5°C/min, and then water quenched. 800°C means the alloy was further annealed at 800°C for 216 h. The data of the equilibrium compositions of the two phases in Ti–48Al–2Nb–2Cr alloy at 1300 and 1000°C were cited from Ref. [28].

experimental evidence of a diffusion field existing around a growing γ tip in the high temperature α matrix of the Ti–44Al alloy [17].

No segregation of Nb, Cr and V elements along the primary α/γ interface of Fig. 4A and B was observed from the reconstructed atom maps of the solute partitioning and the composition profiles across the interface. However, Larson's study pointed out that Cr segregates to certain α_2/γ interfaces [23]. For γ/γ boundary, Cr was found also to segregate some types of boundaries while Nb not [23,25]. A systematic study by Inui et al. [25] using as-grown PST crystals indicates further the segregation of Cr depends on the type of a γ/γ lamellar boundary. It is observed at the 60°- and 120°-rotational boundaries while not at the true-twin boundary.

Usually the segregation of an additive favors to one imperfect interface (the non-coherent or semi-coherent rather than the coherent interface), resulting in the decrease of the system energy [32]. Because of the tetragonality of the $L1_0$ structure of the γ phase, the interfaces corresponding to the twin relationship are fully coherent, whereas those corresponding to the rotational relationship should generate a mismatch [25,26,35]. It is also the similar case for the $\alpha(\alpha_2)/\gamma$ interfaces where many interfacial dislocations were observed [16]. So Cr was usually found to segregate at the α_2/γ and rotational γ/γ boundaries rather than the true-twin γ/γ boundary.

On the other hand, the segregation difference among the additives generally depends on their maximum solubility in a phase, and it has been confirmed experimentally the smaller the maximum solubility of an additive is, the larger the extent of the segregation is [32]. From the isothermal sections in the Ti–Al–Nb and Ti–Al–Cr systems at various temperatures [36–38], it is found Nb has much more solubility than Cr in both $\alpha(\alpha_2)$ and γ phases. Thus, Cr was found to segregated to some α_2/γ and rotational γ/γ boundaries while Nb not, but Cr was not found to segregate to the α/γ interface in our case probably due to the high temperature because the extent of segregation will decrease drastically at a higher temperature [32], or it may be also due to the limit of our observation because the α/γ interface of only about 15 nm in length was examined.

When the alloy was slowly cooled from 1400 to 850°C, it is difficult to observe the α_2/γ interface by FIM because of a quite low amount of the α_2 phase in this alloy which is related to the high Al content of the alloy and a little shift of both the $\alpha_2/(\alpha_2+\gamma)$ and $(\alpha_2+\gamma)/\gamma$ phase boundaries to the Ti-rich side compared with the Ti–Al binary system [28]. In this case, the γ phase is easy to be detected and the AP result shows that except some concentration change of Ti and Al in the γ phase, there is little change for the additives compared with that of the alloy cooled from 1400 to 1300°C. However, if the alloy was further annealed at 800°C for 216 h, Nb and Cr seems to be enriched a little more in the γ phase, which means Nb favors to stabilize the γ phase below the eutectoid temperature while the effect of Cr on the α_2 phase decreases. The result is consistent with that in Ref. [28].

4. Conclusions

After a Ti–47Al–2Nb–1Cr–1V alloy was solution treated and then cooled to 1300°C at a rate of 50°C/min, or cooled to 850°C at 5°C/min and further annealed at 800°C for 216 h, a fully $\alpha(\alpha_2)/\gamma$ lamellar structure was obtained. The AP results show that V and Cr, and interstitial elements C and O are enriched in the high-temperature α phase, while Nb is almost homogeneous in the two phases. No segregation of Nb, Cr and V elements along the examined high-temperature α/γ interface was observed from the reconstructed atom maps of the solute partitioning. The EELS result is qualitatively consistent with that of the AP microanalysis.

Acknowledgements

G.W.Q is very grateful to the Royal Society of the UK for the financial support (ART/CAN/SV/EXQ(1)). G.W.Q. would also like to appreciate Professor J. Titchmarsh, Drs. S. Kim, P.J.S. Warren and M. Huang for helpful discussion, and Mr. T. Godfrey for technical assistance at the University of Oxford.

References

[1] Maziasz PJ, Liu CT. Metall Mater Trans A 1998;29A:105.
[2] Froes FH. JOM 1989;41(6):6.
[3] Appel F, Wagner R. Mater Sci Eng 1998;R22:187.
[4] Yamaguchi M, Inui H, Ito K. Acta Mater 2000;48:307.
[5] Kim YW, Dimiduk DM. In: Proc. JIMS, High temperature deformation and fracture. Sendai (Japan): JIM, 1993. p. 373.
[6] Frommeyer G, Wunderlich W, Kremser Th, Liu ZG. Mater Sci Eng 1995;152A:116.
[7] Clemens H. Z Metallkd 1995;86(12):814.
[8] Kim YW. Acta Metall Mater 1992;40(6):1121.
[9] Qin GW, Hao SM, Han CX. J Mater Sci Tech 1997;13(6):452.
[10] Es-Souni M, Wagner R, Beaven PA. Mater Sci Eng 1992;153A:444.
[11] Kim BG, Kim GM, Kim ChJ. Script Metall Mater 1995;33(7):1117.
[12] Jones SA, Kaufman MJ. Acta Metall Mater 1993;41:387.
[13] Denquin A, Naka S. J Phys III Coll 1993;C73:383.
[14] Qin GW, Hao SM, Song D. Acta Mater Sinica 1998;34(10):1279.
[15] Denquin A, Naka S. Acta Mater 1996;44(1):343.
[16] Qin GW, Hao SM, Sun XD. Script Mater 1998;39(3):289.
[17] Tanimura M, Inoue Y, Koyama Y. Script Mater 1998;39(7):907.
[18] Mahon GJ, Howe JW. Metal Trans A 1990;21A:1655.
[19] Pond RC, Shang P, Cheng TT, Aindow M. Acta Mater 2000;48:1047.

[20] Hono K, Abe E, Kumagai T, Harada H. Script Mater. 1996;34: 495.
[21] Denquin A, Naka S, Huguet A, Menand A. Script Metall Mater 1993;28:1131.
[22] Kim S, Smith GDW, Roberts SG, Cerezo A. Mater Sci Eng 1998;250A:77.
[23] Larson DJ, Liu CT, Miller MK. Mater Sci Eng 1997;A239–240: 220.
[24] Hu D, Godfrey AB, Lorreto MH. Intermetallics 1998;6:413.
[25] Inui H, Kishida K, Kobayashi M, Yamaguchi M. Phil Mag A 1996;74(2):451.
[26] Ito K, Vitek V. Acta Mater 1998;46:5435.
[27] Livingston JD, Cahn JW. Acta Metall Mater 1974;22:495.
[28] Qin GW, Hao SM, Zeng NH. Acta Metall Sinica 1995;31(11): B484.
[29] Huang SC, Hall EL. In: Liu CT, editor. High temperature ordered intermetallic alloys. Pittsburgh, MRS, 1989. p. 391.
[30] Kim YW. J Metall 1989;41:24.
[31] Hillert M. In: Hillert M, editor. Diffusion and thermodynamics in alloys. Beijing (China) Metallurgical Industry Press, 1981. p. 260 (in Chinese).
[32] Xiao JM. In: Xiao JM, editor. Phase and phase transformations in alloys. Beijing (China): Metallurgical Industry Press, 1987. p. 240–313 (in Chinese).
[33] Ding JJ, Zhao G, Hao SM. Acta Metall Sinica 1997;33(10): 1105 (in Chinese).
[34] Semiatin SL, Seetharaman V, Dimiduk DM, Ashbee KHG. Metall Mater Trans A 1998;29A(1):7.
[35] Zghal S, Naka S, Court A. Acta Mater 1997;45:3005.
[36] Wang XT, Chen GL, Ni KQ, Hao SM. J Phase Equilibria 1998;19(3):200.
[37] Nakamura H, Takeyama M, Yamab Y, Kikuchi M. Script Metall Mater 1993;28:997.
[38] Hayes FH. J Phase Equilibria 1992;13(1):79.